Polymer Chemistry

Accepted Manuscript

ROYAL SOCIETY OF CHEMISTRY

www.rsc.org/polymers

Journal Name

RSCPublishing

ARTICLE

Enhanced drug toxicity by conjugation of platinum drugs to polymers with guanidine containing zwitterionic functional groups that mimic cell-penetrating peptides

Cite this: DOI: 10.1039/x0xx00000x

Received ooth January 2012,
Accepted ooth January 2012

DOI: 10.1039/x0xx00000x

www.rsc.org/

Khairil Juhanni Abd Karim,[a,b] Robert H. Utama,[a] Hongxu Lu,[a] Martina H. Stenzel[a],

Inspired by the Ringsdorf model, statistical copolymers with solubility enhancers, platinum drugs and groove binders were compared. In addition, the polymer was furnished with a cell penetrating moiety using a guanidine containing polymer. A block copolymer based on poly(4-vinylbenzyl chloride) and a block carrying zwitterionic monomer prepared from arginine was obtained using RAFT polymerization. Thiol-chloride reaction was then employed to attach thioglycerol (TG) as the water-soluble functional group, 9-aminoacridine (AA) as groove binder to enhance DNA binding and reactive diamino functionality as the bidendate ligand for the conjugation of platinum drugs. The aim of this work was to create a stable bond between the polymer and the drug to answer the question if it is essential to have degradable linkers to generate high drug activity. Three platinated polymers - having only the solubility enhancer, the solubility enhancer and the groove binder and with all three moieties- were compared in regards to their ability to enter the human ovarian carcinoma A2780 cells. Unsurprisingly, the zwitterionic polymer showed the highest uptake, which also coincided with a higher toxicity of the drug. Conjugated to the zwitterionic polymer, the platinum drug showed a higher toxicity than free cisplatin. In summary, even 40 years after the concepts was first established by Ringsdorf, this design still seems to have high validity highlighting that the suitable polymer design can enhance the activity of the drug.

Introduction

Platinum drugs are widely applied to treat cancer despite their significant side effects.[1, 2] Their activity is based on their ability to bind to the DNA causing damage to the cell. Most platinum drugs have a similar base structure in common, which encompasses two permanent, usually amine based, ligands and two labile ligands, often chlorides or carboxylates, which can be replaced by water. Oxidation of platinum drugs to a higher oxidation state leads to prodrugs that are typically less toxic, but they need to be reduced in the reductive cell environment in order to be active.[3] The delivery of platinum drugs using polymers or other nano-sized carriers is now an established field with numerous reports in the literature.[4] Different pathways have been described including the physical encapsulation of the drug, the conjugation using the axial ligands of the platinum(IV) prodrug or the conjugation via the leaving ligands, where the platinum drug is typically attached to polymers with carboxylate groups.[4] The conjugation of the drug *via* the permanent amine ligands has barely been explored and many aspects of this pathway are still a matter of debate. The permanent conjugation of the drug results in the formation of a macromolecular drug. The polymer therefore does not act as a drug carrier *per se*. Instead, a new macromolecular drug with multiple copies has been created. This macromolecular drug needs to enter not only the cell, but also the nucleus in order to bind with the DNA. However, it has been hypothesized in literature that permanently conjugated drugs might not be active and cleavable linkers, such as ester functionalities, are required to achieve high biological activity.[5] This assumption is based on the fact that nuclear pores may have diameters of around 100 nm, but the regulatory system probably only allows molecules of sizes well below 10 nm to freely diffuse in and out. Most macromolecular platinum complexes described so far had indeed degradable groups, either in the backbone or the linker to the drug and therefore size considerations were less important.[6-12] Most polymers were designed in a way that the polymer is partly degradable and additionally aggregated into nano-sized carrier. This makes it impossible to isolate the effects: Inactivity of the conjugated drugs may either be due to insufficient degradation of the polymer or the nano-sized polymer aggregate was too stable and well above the 10 nm cut-off and did not allow penetration into the nucleus.[13] It can certainly be stated that large particles combined with low

degradation of the linker can render the macromolecular drug inactive. Depending on the overall structure of the polymer, esters have been found to be sufficiently labile to ensure good bioactivity.[14] Replacing the ester functionality by an acid-labile hydrazone functionality allowed the triggered liberation of the drug in the acidic cell environment and can enhance the bioactivity of the complex.[15] Degradation of the linker between the drug and the polymer may indeed be the key to high bioactivity. For example, dendrimers with amino end-groups, which can then bind to the platinum(II) chloride species in a stable manner, showed only low toxicity.[16]

We hypothesize that a flexible and soluble linear chain with pendant platinum drugs that may be able to wrap around the DNA will be sufficient to achieve high toxicity. The multiple copies can simultaneously bind to the DNA, but binding can be further advanced using a groove binder such as acridines.[17] The helix structure of the DNA has a major groove, where the twin helical strand is further apart, and a minor groove that is only 12Å wide. Many drugs and dyes bind to the minor groove[18] including intercalating agents.[19] The combination of platinum drugs with a ligand that contains acridine has been shown to lead to successful double attack on cancer cell.[20] Although such polymer with attached acridine may show high DNA binding activity, good cellular uptake needs to be ensured. Linear polymer chains are often only taken up by the cell in a sluggish manner. Alteration of the polymers to enable formation of nanoparticles[21] or the attachment of cell penetrating peptides[22] can aid the cellular uptake of the polymer and with it an increased number of drugs. Examples of cell-penetrating peptides include the guanidinium-rich transporters (GRT).[23] The ability to enhance cell uptake was assigned to the presence of arginine, which contains guanidine groups. Several reports in literature use either the peptide oligoarginine[24-26] or a synthetic version to facilitate the transport of the macromolecular drug into the cell.[23, 27, 28] Recently, a zwitterionic polymer based on arginine was identified as an efficient drug transporter that, at the same time, does not show any toxicity.[29]

In this work, we consciously chose a non-degradable linker to highlight that the drug does not have to be liberated for its activity as long as the polymer meets sufficient criteria, such as small size and high cellular uptake. We therefore hypothesize that a polymer inspired by the Ringsdorf model,[30] that proposes the use of multifunctional polymers with pendant drugs, solubility enhancers and cell-penetrating or targeting ligands, may be sufficient to achieve high bioactivity.[31] In contrast to the Ringsdorf model that recommends a degradable linker between polymer and drug, the drug here is attached in a permanent fashion using thiol-click reaction [32, 33] to eliminate the possibility of degradation and to create a true macromolecular drug. Thioglycerol (TG) will be employed as solubility enhancer while SH-DAP-BOC will act as the permanent ligand for the platinum drug. The drug will therefore be randomly distributed along the polymer chain. The intercalating dye, 9-aminoacridne (AA) will enhance and prolong binding of the polymer to the DNA (**Scheme 1**). These statistical polymer structures will be complemented by polymer C that carries a zwitterionic polymer block, which will simulate the cell-penetrating peptide oligoarginine. Three different polymers were prepared and initial *in-vitro* results were presented in this communication.

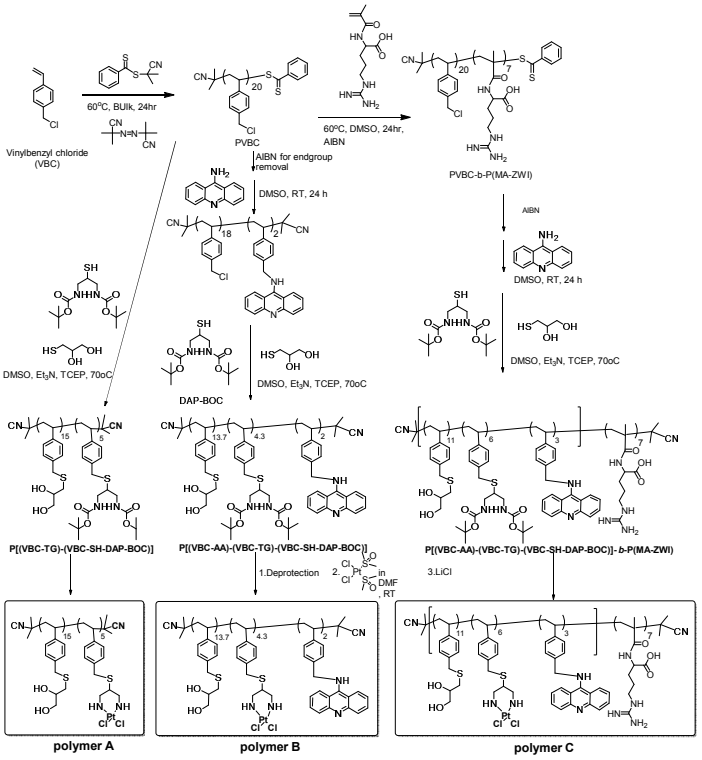

Scheme 1. Synthesis approach of three different types of polymers with pendant platinum drugs

Experimental

Materials

The following chemicals below and are used as received unless stated otherwise. 4-Vinylbenzyl chloride (VBC, Aldrich), 1-thioglycerol (TG, Sigma, 99%), tris(2-carboxyethyl)phosphine (TCEP, Sigma), *N,N*-dimethylacetamide (DMAc; Aldrich, 99.9%), dimethylsulfoxide (DMSO; Ajax, 98.9%), potassium thioacetate and anhydrous methanol (Aldrich) were used without any further purification. 2,2'-Azobisisobutyronitrile (AIBN) was dissolved and recrystallized from methanol. The RAFT agent, 2-cyanopropyldithiobenzoate (CPDB) was synthesized according to literature.[34] The synthesis of BOC-protected 1,3-diaminopropan-2-ol and the mesylation (MS-Cl) was described elsewhere.[14]

Synthesis and Procedures

Synthesis of O-(2,2,12,12-tetramethyl-4,10-dioxo-3,11-dioxa-5,9-diazatridecan-7-yl) thioacetate (Thiolacetyl-DAP-BOC)

MS-Cl (5 g, 1.12 x 10^{-2} mol) and potassium thioacetate (1.93 g, 1.69 x 10^{-2} mol) were dissolved in dry acetone (25 mL). The reaction was carried out under reflux, with constant stirring, for 48 hours. After 24 hours of reaction, one equivalent of potassium thioacetate was introduced and the reaction was stirred for another 24 hours. After the reaction was completed, the mixture was cooled to room temperature and the solvent was removed under reduced pressure. Excess potassium thioacetate was then removed by dissolving the crude product in diethyl ether, followed by filtration. The solvent was then

removed under pressure and the residue was purified by silica gel chromatography, using solvent mixtures of DCM:methanol (98:2 v/v ratio, product TLC R_f = 0.45), yielding thiolacetyl-DAP-BOC as a light brown solid (yield 65%). The purity of the product was obtained using ^{1}H NMR.
^{1}H NMR ($CDCl_3$, 300 MHz) δ 1.44 (s, 18H, $COOC(CH_3)_3$), 2.38 (s, 3H, SC(O)CH3), 3.15-3.45 (m, 4H, $CHCH_2COO$), 3.53 (m, 1H, C*H*), 5.3 (br s, 2H, N*H*).

Synthesis of di-tert-butyl (2-mercaptopropane-1,3-diyl) dicarbamate (Thiol-DAP-BOC, SH-DAP-BOC)
Thiolacetyl-DAP-BOC (1 g, 3.23 x 10^{-3} mol) was dissolved in anhydrous methanol (20 ml) inside the glove box. A solution (20% w/w) of methanolic potassium hydroxide (5.63 mL, 3.25 x 10^{-2} mol) was added under stirring. The reaction was carried out under dry conditions at room temperature for twenty four hours. At the completion of the reaction, the solution was acidified (pH of 6) with glacial acetic acid and the solvent was removed under reduced pressure. The residue was redissolved in water (20 mL) and the product was extracted with chloroform (100 mL). The aqueous layer was washed further three times and the organic layers were all combined and dried over magnesium sulphate. Magnesium sulphate was then removed using filtration and the solvent was removed under reduced pressure, yielding (70%) the product at high purity.
^{1}H NMR ($CDCl_3$, 300 MHz) δ 0.8 (s, 1H, CHS*H*), 1.43 (s, 18H, $C(CH_3)_3$), 2.86-3.13 (3H, $C(CH_2)CH$SH), 5.3 (br s, 2H, NH).

RAFT polymerization of Poly(vinylbenzyl chloride), PVBC
In a reaction vial, CPDB (157.2 mg, 7.10 x 10^{-4} mol) and AIBN (11.7 mg, 7.10 x 10^{-5} mol) were dissolved in vinylbenzyl chloride (10 ml, 7.10 x 10^{-2} mol) and purged with N_2 for 40 minutes. The reaction mixture was heated at 60°C for 24 hours. The vial is then exposed to air to stop the polymerization and the polymer was purified by precipitation in methanol. The polymers were analysed *via* ^{1}H NMR and GPC. (Conversion = 20%, M_n = 5400 gmol^{-1}, Đ = 1.16).
^{1}H NMR (300 MHz, DMSO-d6, 25 °C): δ (ppm) = 1.2-1.7 (1H, $CH_2CHC(CH)_2(CH)_2CCH_2Cl$ + 2H, $CH_2CHC(CH)_2(CH)_2CCH_2Cl$), 4.6 (2H, $CH_2CHC(CH)_2(CH)_2CCH_2Cl$), 6.5 (1H, $CH_2CHC(CH)_2(CH)_2CCH_2Cl$); 7.1 (t, 1H, $CH_2CHC(CH)_2(CH)_2CCH_2Cl$)

Synthesis of Arginine-Methacrylate Monomer, Ma-ZWI [29, 35]
Arginine hydrochloride (4.2 g, 0.02 mol) was dissolved with sodium hydrogen carbonate (3.36 g, 0.04 mol) in 20 mL water. The solution was cooled to 5°C and methacrylic anhydride (3.4 ml, 0.022 mol) was added drop-wise over a period of 10 minutes. The mixture was stirred at 5°C for 6 hours. A few drops of concentrated HCl were added to adjust the pH to 7. The monomer is then dissolved in DMSO and freeze-dried. (Yield : 40%)
^{1}H NMR (300.17MHz, DMSO-d6, 25 °C): δ (ppm) = 9.22 (t, 1H, CH_2COO**H**,); 7.73 (t, 1H, CH_2N**H**$_2$CNH,); 5.57 (s, 1H, CC**H**) ; 5.00 (s, 1H, CC**H**) ; 3.90 (m, 1H, NHC**H**) ;1.87 (s, 3H, C**H**$_3$) ; 1.32 (m, 4H, $NHCH_2C$**H**$_2$) .

PVBC-b-P(Ma-ZWI)
The monomer arginine methacrylate (MA-ZWI) (1.9 x 10^{-2} g, 1.39 x 10^{-4} mol) was mixed with the PVBC macroRAFT agent (1.0 x 10^{-1} g, 6.97 x 10^{-6} mol) and AIBN (1.2 x 10^{-4} g, 1.4 x 10^{-6} mol) in 5 mL of DMSO. The solution was degassed with nitrogen for 30 min and the polymerization was carried out at 70 °C for 24 hours. The polymer was purified by dialysis against distilled water with 3500 MWCO membranes over 2 days. The Polymer was freeze dried and stored at -7 °C. Conversion was obtained using ^{1}H NMR (Conversion = 35%).

Removal of RAFT-ends Groups
Into a RAFT polymer (0.1g, 3.3 x 10^{-5} mol) solution in DMSO (5 ml), excess amount of AIBN (20 equivalent to RAFT groups, 0.11g, 6.5 x 10^{-4} mol) was added. The solution was purged with nitrogen gas and reacted at 70 °C overnight. After the reaction, the polymer was precipitated in methanol and the white powder was isolated. The product was analyzed by ^{1}HSQC NMR spectroscopy.
^{1}HSQC NMR (300 MHz, DMSO-d6, 25 °C): δ (ppm) = 1.2 (2H, C**H**$_2$CHC(CH)$_2$(CH)$_2$CCH$_2$Cl), 1.4 and 1.6 (AIBN end groups of PVBC), 1.7 (1H, CH_2C**H**$C(CH)_2(CH)_2CCH_2Cl$), 4.6 (2H, $CH_2CHC(CH)_2(CH)_2CC$**H**$_2$Cl), 6.5 (1H, $CH_2CHC(CH)_2(C$**H**$)_2CCH_2Cl$); 7.1 (t, 1H, $CH_2CHC(C$**H**$)_2(CH)_2CCH_2Cl$)

Thiol-chloride reactions
PVBC (1.5 x 10^{-2} g, 5.0 x 10^{-3} ml, 3.0 x 10^{-6} mol) was dissolved in DMSO-d6 and reacted with 9-aminoacridine (AA, 0.2 eq mol ratio to the available chloride, 0.2 x 10^{-3} g, 10.0 x 10^{-7} mol) in the presence of triethylamine (eq. moles with AA, 0.1 x 10^{-3} g, 10.0 x 10^{-7} mol). The reaction was allowed to proceed at room temperature overnight, which was followed by ^{1}H NMR. The product was purify *via* dialysis against deionized water for 24 hours and freeze-dried to obtain a yellow solid, PVBC-AA. (Conversion = 50% = 2 units).
^{1}HSQC NMR (300 MHz, DMSO-d6, 25 °C): δ (ppm) = 1.7 (2H, C**H**$_2$CHC(CH)$_2$(CH)$_2$CCH$_2$Cl), 4.6 (2H, $CH_2CHC(CH)_2(CH)_2CC$**H**$_2$Cl), 4.4 (2H, $CH_2CHC(CH)_2(CH)_2CC$**H**$_2$-aminoacridine), 6.5 (1H, $CH_2CHC(CH)_2(C$**H**$)_2CCH_2Cl$ + $CH_2CHC(CH)_2(C$**H**$)_2CCH_2$-aminoacridine), 7.1 (t, 1H, $CH_2CHC(C$**H**$)_2(CH)_2CCH_2Cl$ + $CH_2CHC(CH)_2(C$**H**$)_2CCH_2$-aminoacridine), 7.5-8.8 (4H, aminoacridine)

PVBC-AA (1.5 x 10^{-2} g, 5.0 x 10^{-6} mol) was dissolved in DMSO-d6 and thioglycerol (0.9 eq. mol ratio to available chloride, 0.3 x 10^{-3} g, 0.3 x 10^{-3} ml, 3.0 x 10^{-6} mol), SH-DAP-BOC (0.3 eq. mol ratio to available chloride, 0.4 x 10^{-3} g, 1.5 x 10^{-6} mol), triethylamine (eq. moles to available chloride, 0.4 x 10^{-3} g, 0.6 x 10^{-3} ml, 4.4 x 10^{-6} mol) and TCEP (eq. moles to SH-DAP-BOC, 0.4 x 10^{-3} g, 1.5 x 10^{-6} mol) were added. The reaction was heated to 70°C and the product was purified *via* dialysis against deionized water. The product was analyzed by ^{1}H NMR spectroscopy. (Conversion for thioglycerol = 76% = 13.7 units, conversion for SH-DAP-BOC = 72% = 4.3 units)
^{1}H NMR (300 MHz, DMSO-d6, 25°C): δ (ppm) = 1.7 (2H, C**H**$_2$CHC(CH)$_2$(CH)$_2$CCH$_2$Cl), 1.3 and 3.1 (SH-DAP-BOC), 2.3 and 3.5 (thiolgycerol), 3.4 (1H,-O**H** of thioglycerol) 4.4 (2H, $CH_2CHC(CH)_2(CH)_2CC$**H**$_2$-thiogylcerol + $CH_2CHC(CH)_2(CH)_2CC$**H**$_2$-SH-DAP-BOC), 6.5 (1H, $CH_2CHC(CH)_2(C$**H**$)_2CCH_2$-thioglycerol + $CH_2CHC(CH)_2(C$**H**$)_2CCH_2$-SH-DAP-BOC), 7.1 (1H, $CH_2CHC(C$**H**$)_2(CH)_2CCH_2$-thioglycerol + $CH_2CHC(C$**H**$)_2(CH)_2CCH_2$-SH-DAP-BOC)

Synthesis of Platinum-DMSO Complex, $Pt(DMSO)_2Cl_2$
The synthesis of the platinum-DMSO complex was based on literature. [36] Potassium tetrachloroplatinate, K_2PtCl_4 (0.30 g, 7.29 × 10^{-4} mol) was weighed in a *via*l and dissolved in 5 ml of

deionized water. DMSO (0.16 ml, 2.18×10^{-3} mol) was added and the mixture was allowed to stand at room temperature for 30 minutes to 1 hour. Colour change from red to yellow was observed. Formation of yellow crystals was observed after 15 minutes. The crystals were filtered, washed with deionized water (DI), ethanol and dried in vacuum. The crystals were analysed using ^{195}Pt NMR spectroscopy. Pure yellow crystals were obtained with a yield of 0.20 g (65%).
^{195}Pt NMR (DMF/D_2O) = -3645 ppm.

Removal of Amine Protection Groups
Copolymers with *N*-BOC protected ligands were dissolved in anhydrous DCM and degassed for 10 minutes. A few drops of 2M hydrochloride in diethyl ether were added to the solution under constant stirring. The reaction was carried out at room temperature for 24 hours. The solvent was evaporated and the product was purified by washing with diethyl ether. The product was then dried to obtain pure copolymers with active conjugation sites as yellow gel. Successful reaction was confirmed using ^{1}H-NMR by the disappearance of the proton signal at 1.3 ppm, which corresponds to the BOC protective group.

Conjugation of Platinum-DMSO Complex on Copolymers
Copolymers with active conjugation sites were dissolved in DMF and 1 mol eq. of $Pt(DMSO)_2Cl_2$ complex was added. The reaction was let stirred for 24 hours at room temperature. Lithium chloride (5 mol eq.) was added into the solution and reacted for another 6 hours at 80°C. The reaction mixture was cooled to ambient temperature and purified *via* dialysis (MWCO 3500) against DI water using over 2 days. After freeze-drying, the dried brown solid of Pt-conjugated copolymers were obtained. TGA was used to determine the platinum content on the copolymer.

Preparation of Polymeric Nanoparticles via Nanoprecipitation.
Platinated polymer was initially dissolved in 20vol% (of the total volume of solvent) DMF. Deionized water (80vol% of the total volume of solvent to give [Pt] = 100 μM) was added dropwise (0.5 ml/h). Upon the completion, the solution was then dialyzed against deionized water for 1 day to yield the desired nanoparticles. It should be noted here that the aqueous solution replaced at least one of the chloride ligands by water.

In vitro Cell Culture Assays
Human ovarian carcinoma A2780 cells were cultured in T-25 cell culture flasks at 37 °C under an atmosphere of 5 % CO_2. The cell culture medium was composed of RPMI 1640 medium supplemented with 10 % fetal bovine serum, 4 mM glutamine, 100 U/mL penicillin, 100 μg mL^{-1} streptomycin and 1 mM sodium pyruvate. After reaching confluent, the cells were washed with phosphate buffered saline (PBS) and treated with trypsin/EDTA treatment. PBS was composed of 2.7 mM KCl, 1.5 mM KH_2PO_4, 136.9 mM NaCl and 8.9 mM $Na_2HPO_4 \cdot 7H_2O$ and the pH was adjusted to 7.4. The detached cells were collected by centrifugation and resuspended in cell culture medium. The cell suspension was used for the evaluation of cellular responses.

Uptake analysis of polymer
A2780 cells were seeded in a 35 mm Fluorodish (World Precision Instruments) at a density of 60, 000 per dish and cultured for three days with cell culture medium. Samples were loaded to the cells at a working concentration of 50 μg mL^{-1} polymer and incubated at 37 °C for 6 hours. All the samples in the cell culture work were sterilised by UV irradiation for 30 min with sonication in a biosafety cabinet before loading into the cells. After incubation, the cells were washed thrice with PBS and stained with 100 nM LysoTracker Red DND-99 (Invitrogen) for one minute. The dye solution was quickly removed and the cells were gently rinsed with PBS. The dishes were mounted in PBS and observed under a laser scanning confocal microscope system (Zeiss LSM 780).

Determination of Pt content within cells
A2780 cells were seeded in six well cell culture plates and incubated at 37 °C with 5 % CO_2 for 1 day prior to treatment. The medium was replaced with 3 mL fresh media containing each sample (20 μM Pt) at 37 °C for 2 hours. The cell monolayer was washed five times with cold PBS and treated with trypsin/EDTA to detach the cells. The cells were collected by centrifugation and digested with 200 μL 1 N HNO_3 at 60 ºC for 24 hour. Then the lysate was diluted to 10 mL with MilliQ water and the Pt concentration was determined using Inductively Coupled Plasma Mass Spectrometry (ICP-MS).

Cytotoxicity Evaluation
A2780 cells were seeded in 35 mm glass bottom Fluoro dish at 50,000 cells per dish and cultured at 37 °C for one day. After UV sterilisation, the samples were added to the cells at a Pt concentration of 10 μM. After incubation for 1 day, cells were washed with PBS, stained with Hoechst 33342 and observed under an inversed fluorescence microscope. The cell number was calculated based on the microphotographs using ImageJ. Each polymer had 3 parallel dishes. 3 sections of each dish were randomly selected and imaged. Totally, 9 images were used to calculate cell numbers. A One Way Analysis of Variance (ANOVA) was used to reveal the statistical differences followed by a Tukey's test for multiple comparisons.

The cytotoxicity of the polymers was measured using a WST-1 based assay. A2780 cells were seeded into 96-well tissue culture plates at a density of 4,000 cells per well and cultured for 1 day before adding polymers. Polymer A, B or C were dissolved in DMSO and loaded into the cells in the microplates. The DMSO working concentration was 1% and cells cultured with 1% DMSO are used as controls. After 1 day incubation with polymers, the medium containing polymers were discarded and the cells were rinsed with PBS once. Then the cells were cultured with 100 μL medium supplemented with 10 μL WST-1 per well for 3 hr. The absorbance was measured at 450 nm with a reference wavelength at 650 nm and the cell viability was calculated.

Analysis

NMR analysis
^{1}H NMR spectroscopy was used to analyse the synthesized molecules and the copolymers before and after modifications using $CDCl_3$ or DMSO-d6 *via* a 300 MHz Bruker spectrometer. ^{195}Pt-NMR is obtained by dissolving the platinated compound in DMF and the signal was locked with deuterium oxide, D_2O in 400 MHz Bruker.

Gel permeation chromatography (GPC)

The molecular weight distributions and polydispersity index (Đ) of the polymers were analysed *via* Shimadzu modular LC system GPC, comprised of an SIL-10AD auto-injector, LC-10AT pump, a DGU-12A degasser, CTO-10A column oven and an RID-10A differential refractive index detector. Column arrangement comprising of a Polymer Laboratories 5.0 µm bead size guard column (50 × 7.8 mm), followed by four linear PL column (300 × 7.8 mm, 500, 10^3, 10^4 and 10^5 Å, 5 µm pore size) was used for the analysis. The polymer was dissolved in *N,N*-dimethylacetamide (DMAc) at a concentration of approximately 1 mg mL^{-1}. This solution was then filtered through a 0.45 µm PTFE syringe filters.

Dynamic Light Scattering (DLS)
The hydrodynamic diameter was determined using a Zetasizer Nano ZS (Malvern), with a 4 mV He-Ne laser operating at λ = 632 nm and non-invasive backscatter detection at 173°. Measurements were conducted in either Quartz (for organic solvents) or disposable PS (for water) cuvette at 25°C, with 30 s equilibration period prior to each set of measurements. For a given sample, a total of three measurements were conducted. In each measurement, the number of runs, attenuator and path length used were automatically adjusted by the instrument, depending on the quality of the sample. The presented results are averages of the three measurements.

Scanning confocal microscopy
Cellular uptake was studied using a Zeiss LSM 780 Scanning confocal microscope system. The system equipped with a Diode 405-30 laser, an argon laser and a DPSS 561-10 laser connected to a Zeiss Axio Observer.Z1 inverted microscope. The ZEN2012 imaging software (Zeiss) was used for image acquisition and processing. The cellular uptake was observed with a 100 × 1.4 NA oil objective and the cytotoxicity was observed with a 20 × 0.8 NA air objective.

Transmission Electron Microscopy (TEM)
TEM micrographs were obtained using a JEOL1400 TEM operating at an accelerating voltage of 120 kV. Images were recorded via the Gatan CCD imaging software. All TEM samples were prepared by dropping a 1 mg ml^{-1} emulsion on a formvar supported copper grid. Excess solvent was drained using filter paper after 1 min.

Thermogravimetric Analysis (TGA)
The thermal decomposition profiles of the platinated copolymers were obtained using a Perkin-Elmer Thermogravimetric Analyzer (Pyris 1 TGA). Analysis was conducted under air/N_2 atmosphere in a ceramic-reinforced titanium plate. The measurement was carried out over a temperature range from 25 to 600°C with a temperature increment of 10°C/min

Fluorescence Spectroscopy
Fluorescence measurements were performed on Agilent Cary Eclipse Fluorescence Spectrometer using a 1 cm quartz cuvette. Fluorescence spectra were recorded between 400-800 nm at λ_{ex} = 422 nm, λ_{em} = 455 nm with entrance and exit slit width of 5mm.

Results and discussion

Prior to any thiol click reactions, a thiol-functionalised ligand was synthesised. The synthesis of this ligand, SH-DAP-BOC involved a 2-step reaction, following the synthesis route described by Kane *et al.* which is shown in **Scheme 2.**[37] The commercially available 1,3-diaminopropan-2-ol (DAP) has been converted into methanesulfonated DAP-BOC (MS-DAP-BOC). The methanesulfonyl group undergoes nucleophilic substitution with thiolacetate salt in acetone under reflux conditions. The thiolacetate product is then hydrolysed to thiol by the addition of a methanolic potassium hydroxide solution to afford a solid pale-brown product. The compounds obtained was characterised using ^{1}H NMR.

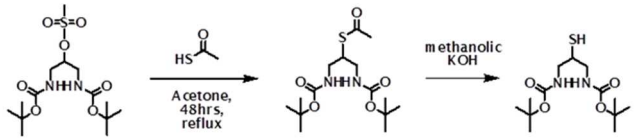

Scheme 2 Synthesis of 1,3-diaminopropane-2-thiol (Thiol-DAP-BOC, SH-DAP-BOC)

Figure S1 (ESI) displays the NMR spectra of each intermediate step and the final product. The disappearing of the methyl signal of MS-DAP-BOC (peak **f**) at 3.1 ppm in spectra **[B]** suggested the complete conversion into a thioester. Hydrolysis of this thioester was successful and the reaction was confirmed by the vanishing of signal **g** corresponding to the acetyl compound. The signal corresponding to the methine functionality (-CH-) adjacent to the thiol should theoretically shifts to higher field, but it could not be clearly identified. However, the broadening of signal **c** between 2.8-3.7 ppm suggested that signal **b** was overlapping with **c**. To identify the position of the methane group, HSQC NMR was carried out and the spectrum is pictured in **ESI, Figure S2.** The methane proton could now be clearly identified as a multiplet at 2.85 ppm coupling with the ^{13}C signal at 50 ppm. The product was in addition analysed using FT-IR to confirm the changes in functionality from DAP-BOC (which was reacted with methanesulphone in the first step) to SH-DAP-BOC (**ESI, Figure S3**). After modification, the SH-DAP-BOC obtained showed the characteristic absorption band at approximately 2400 cm^{-1} associated with the stretching vibrations of the free-thiol (-SH) group (**ESI, Figure S3[B]).** Meanwhile, the absorption band of –OH group disappeared, which confirmed that the hydroxyl group has reacted.

Poly(chloromethyl styrene) or poly(vinylbenzyl chloride), PVBC was chosen as the reactive substrate. The monomer VBC is easily polymerised *via* RAFT polymerization in bulk leading to a polymer with chloride functionalities. Although bromides are in general more reactive than chlorides the neighbouring benzyl groups introduces an unexpected reactivity in S_N2 reactions. In addition, VBC can be easily polymerized *via* RAFT polymerization without any visible signs of chain transfer to chloride.[38] In contrast, bromides are known to undergo substantial chain transfer reactions. PVBC has already been shown to be successful in the reaction with thiols[39]. VBC was subsequently polymerized at 60°C at a monomer to RAFT agent ratio of 100 for 24 hours yielding 20 units of PVBC (**Figure S4**). To alleviate any side-reactions occurring in polymers during the subsequent reactions, the RAFT end groups were removed using AIBN following a procedure established by Perrier and co-workers (**Scheme 1**).[40] The

resulting polymer was colourless (**ESI, Figure S5**). Successful modification was confirmed using HSQC 2D NMR (**ESI, Figure S5**). In addition, no changes in molecular weight and molecular weight distribution were observed (**Figure 1**).

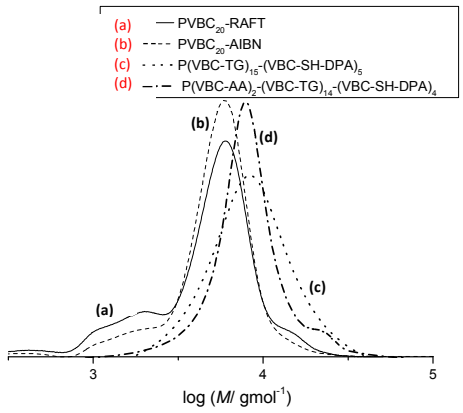

Figure 1 Molecular weight distributions measured by DMAc GPC of (a) PVBC-RAFT, b) PVBC-AIBN (after removal of RAFT end-group), (c) BOC-deprotected $P(VBC\text{-}TG)_{15}$-$(VBC\text{-}SH\text{-}DAP)_5$) and (d) BOC-deprotected $P(VBC\text{-}AA)_2$-$(VBC\text{-}TG)_{14}$-$(VBC\text{-}SH\text{-}DAP)_4$. Both polymers (c) and (d) are prior to platinum conjugation.

Two pathways were investigated to create polymers with TG, AA and SH-DAP-BOC pendant groups. Initially, PVBC together with AA, TG and SH-DAP-BOC were combined in one-pot under basic conditions. Triethylamine (TEA) provides mild basic reaction condition to create the more active thiolate.[41, 42] TCEP was also added to prevent disulphide formation between the thiol compounds. The reaction mixture was heated at 70 °C and the conversion was monitored using ^{1}H NMR over 4 days. However, the characterisations via ^{1}H NMR showed the attachment of TG and SH-DAP-BOC only, but no signals corresponding to AA were observed. In addition, fluorescence analysis, which should reveal the presence of AA, showed only a negligible presence of AA. It was concluded that the reaction with thiols, which were used in excess, was faster than the nucleophilic substitution with amines.

Therefore, an alternative pathway was employed as outlined in **Scheme 1**. AA reacts readily with chloride in the presence of TEA at ambient temperature. A test reaction between the intercalating agent 9-aminoacridine dye (AA) and 4-vinylbenzyl chloride (VBC) (1:1 molar ratio) in the presence of triethylamine (TEA) was carried out directly in an NMR tube using DMSO-d6. The reaction was directly monitored using ^{1}H NMR (**ESI, Figure S6**). The time required for full conversion of PVBC into PVBC-AA is about 24 to 30 hours. The same reaction condition to attach AA was applied with the $PVBC_{20}$ polymer for 30 hours. The ratio between chloride and amine was however set to 20: 2 to aim at a low concentration of AA in the polymer. The characteristic peaks of AA peaks at 7.5 to 9.0 ppm can be observed using ^{1}H NMR, 2D HSQC NMR as shown in **ESI, Figure S7**.

The attachment of AA could readily be identified by comparison of the FT-IR spectra before and after reaction (**ESI, Figure S8**). The appearance of the bands between 3100-3600 cm^{-1} and 1600-1700 cm^{-1} which is assigned to the frequencies of secondary amines for AA on $P[VBC_{18}\text{-}(VBC\text{-}AA)_2]$ showed that the attachment of AA was successful.

Subsequently, $PVBC_{20}$ or $P[VBC_{18}\text{-}(VBC\text{-}AA)_2]$ were mixed with TG and SH-DAP-BOC in the presence of triethylamine (TEA). TCEP was added to break the disulphide bridge (SH-DAP-BOC had the tendency to dimerize) thus preventing disulfde formation during the reaction at 70 °C. The reaction was carried out in an NMR tube in DMSO-d6 for 4 days. Similar to earlier reactions, the methylene signal at around 4.5 ppm disappeared and the new signal at 4.3 ppm emerged. 80-90% conversion was achieved after 24 hours, but the reaction was allowed to proceed for four days to achieve full conversion. Purification *via* dialysis against deionised water gives a slightly cloudy but stable solution suggesting that the attached TG increased the hydrophilicity. ^{1}H NMR analysis was carried out using deuterated DMSO-D_2O mixture (**Figure 2**). From the ^{1}H NMR spectra the final polymer compositions were $P(VBC\text{-}TG)_{15}$-$(VBC\text{-}SH\text{-}DAP\text{-}BOC)_5$] (polymer A) and $P[(VBC\text{-}AA)_2$-$(VBC\text{-}TG)_{13.7}$-$(VBC\text{-}SH\text{-}DAP\text{-}BOC)_{4.3}]$ (polymer B), respectively.

FT-IR characterisation was carried out to confirm the presence of the functional groups (**ESI, Figure S9).** Most importantly was the disappearance of the C-Cl band at 1260 cm^{-1}. Fluorescence spectroscopy was carried out confirming the presence of AA by comparing the spectra of 9-aminoacridine (AA) with the polymer (**ESI, Figure S10**). The calculated amount of AA conjugated to the polymer was in agreement with the amount determined by NMR and amounts to 2 units per polymer chain.

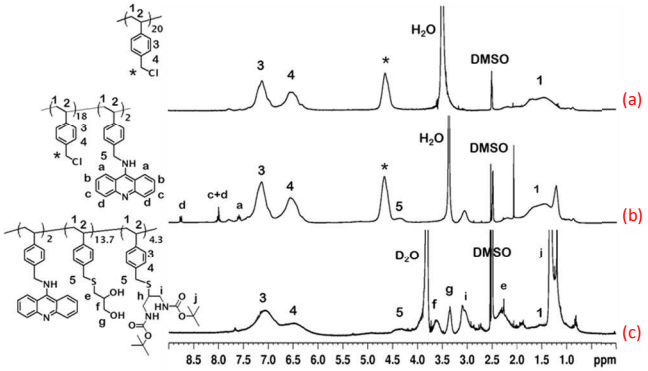

Figure 2 ^{1}H NMR (DMSO-d6) of [a] PVBC, [b] $P[VBC_{18}\text{-}(VBC\text{-}AA)_2]$ and [c] $P[(VBC\text{-}AA)_2$-$(VBC\text{-}TG)_{13.7}$-$(VBC\text{-}SH\text{-}DAP\text{-}BOC)_{4.3}]$.

Due to the fascinating properties of cell-penetrating peptides which can improve the cell uptake of the carrier, chain extension of the PVBC macroRAFT agent with an arginine-functionalised monomer was carried out.[23, 27] The cationic guanidine functionality is known to enhance cell uptake,[23] but can also act as antimicrobial agent[43, 44] or be used for gene delivery.[45] The methacrylate-based and guanidine containing arginine monomer (**Scheme 1**) (MA-ZWI), which was recently shown to enhance cell uptake while being non-toxic[29], was synthesised from arginine hydrochloride and methacrylic anhydride in buffer solution analysed using ^{1}H NMR in DMSO-d6 (**ESI, Figure S11**). The MA-ZWI monomer has a zwitterionic structure in physiological conditions: The guanidine group is protonated while the carboxylic group is

deprotonated. The resulting MA-ZWI is only soluble in water and DMSO, which limits the choice of solvents for the chain extension of PVBC as depicted in **Scheme 1**. During polymerization the solution turned opaque due to the limited solubility of the resulting polymer P(MA-ZWI) in DMSO. Thus, the ^{1}H NMR spectrum of the block copolymer resulted in broad peaks (**Figure 3**). Nevertheless, from the integrations of the proton on the carboxylic acid a block length of 7 units of MA-ZWI was calculated as shown in **ESI, Figure S12.** Similarly to the PVBC homopolymer, P(VBC)$_{20}$-*b*-P(MA-ZWI)$_7$ was reacted with AA intercalating agent first, followed by the reaction with the thiols. **Figure 3** shows the ^{1}H NMR of the block copolymer with the zwitterionic block, P(VBC)$_{20}$-*b*-P(MA-ZWI)$_7$. The four characteristic peaks of AA are observed at 7.3, 7.7, 7.8 and 8.4 ppm. Integration reveals that 3 units of AA are attached. TG and SH-DAP-BOC were reacted in a subsequent step. From the integrations, it can be calculated that 6 units of ligands (SH-DAP-BOC) and 11 units of TG have reacted. The ratio between TG and SH-DAP-BOC is therefore similar to the feed ratio used (molar ratio 3:1). The ratio is also similar to the one obtained after reaction with PVBC homopolymer. The findings were also confirmed *via* FT-IR spectroscopy shown in **ESI, Figure S13**. Due to the limited solubility of these polymers in the GPC solvent, molecular weight characterization was not possible. The zwitterionic polymer block is only soluble in water while the modified PVBC is not sufficiently soluble in the same solvent.

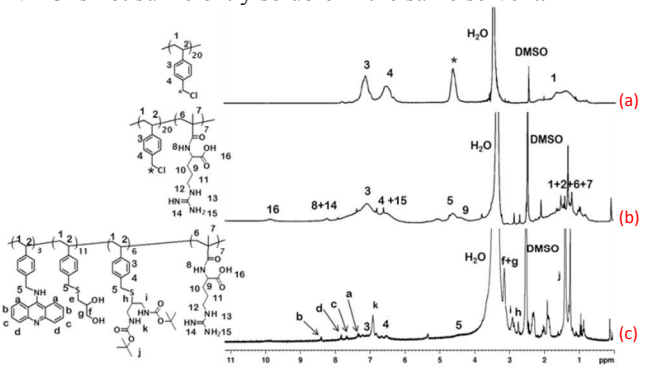

Figure 3 ^{1}H NMR spectra in DMSO-d6 of [a] PVBC, [b] P(VBC)$_{20}$-*b*-P(MA-ZWI)$_7$ and [c] P[(VBC-AA)$_2$-(VBC-TG)$_{11}$-(VBC-SH-DAP-BOC)$_6$]-*b*-P(MA-ZWI)$_7$

The three polymers were deprotected using HCl and subject to the formation of macromolecular platinum complexes. Removal of the BOC groups was evidenced by the disappearance of the BOC signal at 1.3 ppm in ^{1}H NMR. The polymers were now characterized with GPC to identify for any side reactions. Again, the polymer with the zwitterionic structure was not soluble in sufficient amounts to obtain a reasonable GPC signal. Polymer A and B in contrast showed a monomodal molecular weight distribution with a number-average molecular weight M_n of approximately 8,000 g mol^{-1}. (A: 7,700 gmol^{-1}, B: 8,000 gmol^{-1}) (**Figure 1**). Side reactions, that may indicate some polymer-polymer coupling, are absent. The platinum conjugation was subsequently carried out in a similar way as described previously[14] using a 1:1 molar ratio of ligand to platinum complex at ambient temperature for 24 hours. DMF was chosen as solvent to ensure high solubility of the polymer during conjugation. Finally, the polymeric platinum conjugated drug was treated with a fivefold excess of LiCl at 80°C for 6 hours to replace the DMSO ligand with chloride leading to a dark yellow solution of platinum conjugates with dichloro-complex. The solution was purified *via* dialysis against DI water. TGA analysis revealed the amount of conjugated platinum drugs (**Table 1**). The wt% of Pt was then recalculated into the fraction of diamine bidendate ligands that carried a platinum drug. In agreement with earlier work, the conjugation efficiency was almost 100%.[14] The structure is depicted in **Scheme 1**, but the reader needs to consider that the sulphur could partially be involved in the complexation.[46]

The polymers could not directly be dissolved in water at high concentrations and therefore a nanoprecipitation procedure was employed, which involved dissolving the polymer at a low concentration of DMSO followed by slow addition of water and the removal of DMSO by dialysis. The resulting platinum loaded nanoparticles or micelles had sizes between 100 to 500 nm depending on the type of polymer. DLS and TEM (**Table 1, Figure 4**) are in good agreement for polymer A and B, but TEM demonstrated a more regular size distribution of polymer C than DLS may suggest. It is likely that the zwitterionic group have a noticeable tendency to aggregate in aqueous solution. There is obviously no correlation between the type of polymer and the particle size. In addition, the aggregate size is broad indicative of an uncontrolled process and the formation of structures that are not in a thermodynamic equilibrium.

Table 1 Pt-content of each polymer and the fraction of bidentate amino ligands that is conjugated to Pt-drugs in addition to the particle size of the polymers in water at 0.15 mg mL^{-1}

Polymer	Samples	Pt-content (conjugation efficiency)/ %	D_n/nm (DLS)	D_n/nm (TEM)
A	P(VBC-TG)$_{15}$-(VBC-SH-DAP-Pt)$_5$	16 (>95%)	488	200-1800
B	P(VBC-AA)$_2$-(VBC-TG)$_{14}$-(VBC-SH-DAP-Pt)$_4$	15 (>95%)	122	60-200
C	P(VBC-AA)$_3$-(VBC-TG)$_{11}$-(VBC-SH-DAP-Pt)$_6$-*b*-P(MA-ZWI)$_7$	17 (>95%)	250	100-170

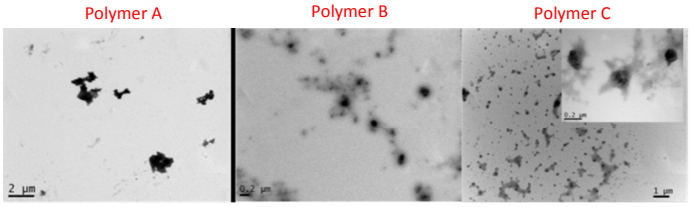

Figure 4 TEM analysis of the platinum loaded polymer A (left), B (middle) and C (right) prepared from an aqueous solution at a concentration of 0.15 mg mL^{-1}

However, the overall high hydrophilicity of the polymer can only lead to loose aggregates **(Figure 5).** While the polymer form aggregates at higher concentrations **(Figure 4)**, these aggregates start disappearing quickly when the solutions were diluted. This aspect is crucial considering that polymers in a drug delivery scenario are subjected to very high dissolution. The following *in-vitro* studies employed solutions with a platinum concentration of 10µM, which was chosen based on the typical IC$_{50}$ values of cisplatin. This platinum concentration equates to a polymer concentration of approximately 0.015 mg mL^{-1} depending on the polymer. The stability of these aggregates was therefore further investigated using DLS. The

scattering intensity was recorded at a fixed aperture, which revealed that the aggregate disassembled at polymer concentrations between 0.02 to 0.04 mg ml^{-1} **(Figure 5).**

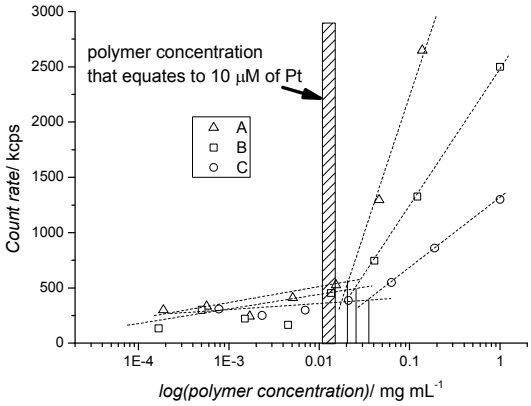

Figure 5 Scattering intensity of the macromolecular platinum drugs in water depending on the concentration

Prior to the toxicity analysis of the polymer, the amount of drug delivered into the cells was investigated. The internalisation of micelles was monitored using confocal fluorescence microscopy. Thanks to the fluorescence of 9-aminoacridine (acridine), the conjugation of a fluorophore to the polymer was not necessary. After incubating the cells with the polymer for 6 hours, the lysosomes were stained with LysoTracker (red) to help identify the location of the nanoparticles. Acridine (yellow) was excited at 405 nm and the emission was monitored at 450 - 500 nm (**Figure 6**). Both, polymer B and C entered the cells and they are partly co-localized with the lysosomes. However, the yellow-green fluorescence of the polymers is not always co-localized with the lysosomes suggesting potentially other uptake mechanism. The detailed mechanism on how the polymers enter the cells is therefore currently unknown. Polymer C seems to be more intense than polymer B indicating that the zwitterionic polymer aided the cell uptake, which is in agreement with earlier studies.[29]

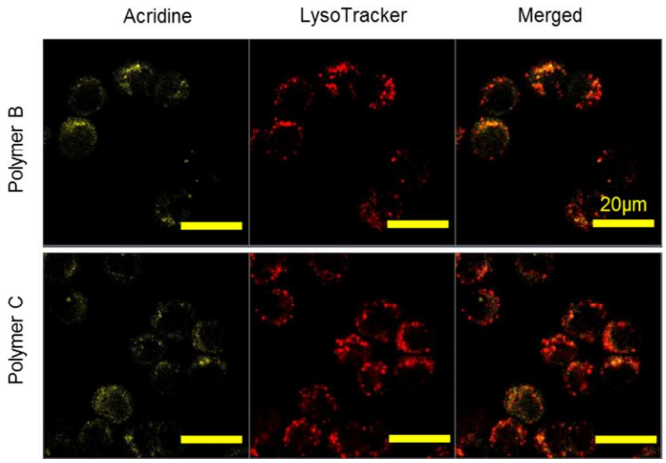

Figure 6 LSCM images of A2780 cells incubated with micelles of polymer B and C for 6 hours. Acridine in the polymer showed the location of micelles (yellow-green). The lysosomes were stained with LysoTracker (Red). Scale bar = 20 μm.

The cells were then digested to measure the amount of platinum inside the cells, which was quantified by ICP-MS (**Table 2**). Polymer A gave irreproducible results, probably caused by the tendency to aggregate, and the sample has therefore not been included. However, it was noted that the uptake was overall lower than any of the other polymer samples. Cisplatin showed the lowest uptake and it seems evident that the polymer could increase the amount of platinum inside the cell even if the polymer did not have any cell penetrating properties. As expected, the zwitterionic structure led to the highest accumulation, highlighting again the ability of these groups to enhance the uptake of the polymer and with it the drug.

Table 2 Uptake amount of Pt per million into A2780 cells measured by ICP-MS

	A	B	C	Cisplatin
[Pt] (ng)	N.A*	31.9 ± 0.7	51.4 ± 1.7	12.7 ± 0.2

*N.A., not available since irreproducible results, but possibly lower than B and C

The cytotoxicity of micelles were tested against A2780 cells and compared with free cisplatin. Cells were seeded in a 35 mm dish and incubated with micelles or drug at a Pt concentration of 10 μM. Prior to the investigation of the cytotoxicity of the macromolecular Pt-drug, the polymers with drugs were tested. As shown in Figure S14, none of the polymers showed toxicity to A2780 cells at the concentration corresponding to 10 μM Pt. From **Figure 7A**, polymer C and cisplatin induced an obvious decrease of cell number. The cell numbers after Pt treatment were measured and plotted in **Figure 7B**. Polymer C displayed the highest toxicity, which correlated to the highest uptake. Polymer B had a lower uptake into the cell, which coincides with a lower toxicity. Polymer A showed the lowest toxicity. The distinguishing feature of this polymer is the absence of a groove binder that can enhance the interaction with the DNA. Better binding of polymer B to the DNA may lead to higher toxicity. However, without any detailed analysis of the precise binding mechanism between acridine and DNA, this can only be subject to speculations. It needs to be considered that modifications to acridine, such as the conjugation to the polymer, can potentially alter the binding strength.[47]

In summary, the better uptake of the macromolecular drug paired with the formation of only loose aggregates that can disassemble when trying to enter the nucleus can directly lead to higher toxicity, which typically coincides with better binding to the DNA.

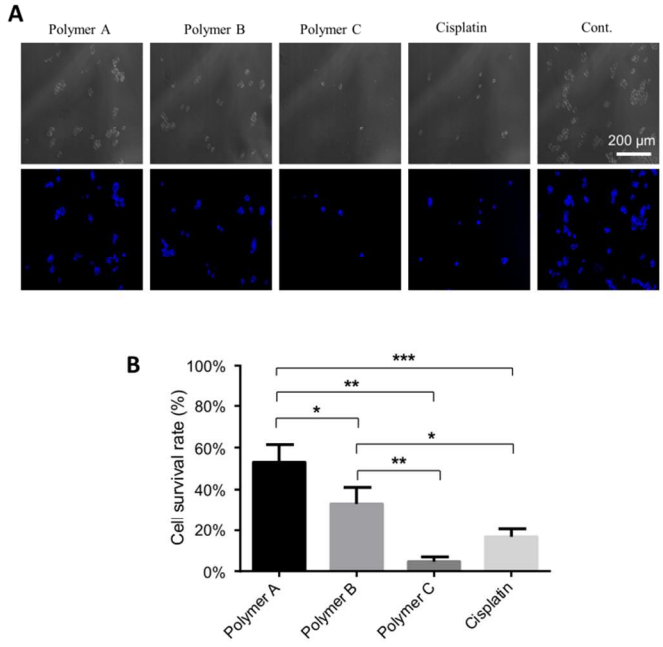

Figure 7. The representative microphotographs of A2780 cells (A) and cell survival rates (B) after treatment with samples for 24 hours. Scale bar in A is 200 µm. B, data represent means ± SD, n =3. ***, significant difference, $p<0.001$. **, significant difference, $p<0.01$. *, significant difference, $p<0.05$.

Conclusions

We generated a set of polymers inspired by the Ringsdorf model that carry the drug as well as solubility enhancers, cell-penetrating properties and other functionalities, here groove binder. The polymers were prepared by postfunctionalization to achieve a random substitution pattern of all the functional groups. The chosen reaction, based on the nucleophilic substitution chlorides with thiols, led to the permanent attachment of the drug. As a result, a macromolecular drug was created whose drug could not be easily cleaved. Purpose was to show that polymer-drug conjugates can be highly effective and the drug does not need to be cleaved from the polymer in order to be active. The key is to create carriers with sufficient solubility that can disassemble into small polymer strands in order to be able to reach the target in the cell. Solubility enhancers such as the attached thioglycerols can assist with this task, but crucial is the attachment of cell-penetrating moieties to ensure high cellular uptake. Groove binders can further enhance the activity if the cellular target is the DNA. In summary, fine-tuning of the properties of the polymer can enhance the activity of the drug resulting in highly efficient macromolecular drugs.

Acknowledgement

MS thanks the ARC (Australian Research Council) for funding in form of a Future Fellowship (FT0991273) and Discovery Projects (DP1092694)

Notes and references

a Centre for Advanced Macromolecular Design, School of Chemistry, University of New South Wales, Sydney 2052, Australia; Tel: +61-2-93854344; E-mail: M.Stenzel@unsw.edu.au
b Department of Chemistry, Faculty of Science, Universiti Teknologi Malaysia (UTM), 81310 UTM Skudai, Johor, Malaysia

.

Electronic Supplementary Information (ESI) available: [details of monomer synthesis and analysis and detailed analysis of polymers]. See DOI: 10.1039/b000000x/

1. L. Kelland, *Nat Rev Cancer*, 2007, **7**, 573-584.
2. S. H. van Rijt and P. J. Sadler, *Drug Discovery Today*, 2009, **14**, 1089-1097.
3. A. V. Klein and T. W. Hambley, *Chem. Rev.*, 2009, **109**, 4911–4920.
4. M. Callari, J. Aldrich-Wright, P. L. de Souza and M. H. Stenzel, *Progr Polym Sci*, **http://dx.doi.org/10.1016/j.progpolymsci.2014.05.002**.
5. V. Delplace, P. Couvreur and J. Nicolas, *Polym Chem*, 2014, **5**, 1529-1544.
6. G. Caldwell, E. W. Neuse and C. E. J. V. Rensburg, *J Inorg Organomet Polym Mater*, 1997, **7**, 217-231.
7. E. W. Neuse, *Polym. Adv. Technol*, 1998, **793**, 786–793.
8. M. T. Johnson, E. W. Neuse, C. E. J. V. Rensburg and E. Kreft *J. Inorg. Organometallic Polym. Mater.*, 2003, **13**, 55-67.
9. G. Caldwell, E. W. Neuse and C. E. J. V. Rensburg, *Appl. Organometallic Chem.*, 1999, **13**, 189–194.
10. W.-C. Shen, K. Beloussow, M. G. Meirim, E. W. Neuse and G. Caldwell, *J. Inorg. Organometallic Polym. Mater.*, 2000, **10**, 51–60.
11. B. Schechter, G. Caldwell, M. G. Meirim and E. W. Neuse, *Appl. Organometallic Chem.*, 2000, **14**, 701–708.
12. E. W. Neuse, N. Mphephu, H. M. Netshifhefhe and M. T. Johnson, *Polym. Adv. Technol.*, 2002, **13**, 884–894.
13. J. R. Tauro and R. A. Gemeinhart, *J. Biomater. Sci.*, 2005, **16**, 1233–1244.
14. J. Karim, S. Binauld, W. Scarano and M. H. Stenzel, *Polym. Chem.*, 2013, **4**, 5542-5554.
15. S. Binauld, W. Scarano and M. H. Stenzel, *Macromolecules*, 2012, **45**, 6989-6999.
16. T. Kapp, A. Dullin and R. Gust, *Bioconjugate Chem.*, 2010, **21**, 328–337.
17. G. Cholewinski, K. Dzierzbicka and A. M. Kolodziejczyk, *Pharmacol Rep*, 2011, **63**, 305-336.
18. C. Zimmer and U. Wähnert, *Progr Biophys Mol Biology*, 1986, **47**, 31-112.
19. S. Neidle and Z. Abraham, *Critical Rev Biochem Mol Biology*, 1984, **17**, 73-121.
20. C. L. Smyre, G. Saluta, T. E. Kute, G. L. Kucera and U. Bierbach, *ACS Med. Chem. Lett.*, 2011, **2**, 870-874.
21. B. Blunden, H. Lu and M. H. Stenzel, *Biomacromolecules*, 2013, **14**, 4177-4188.
22. T. Kapp, A. Dullin and R. Gust, *Bioconjugate chemistry*, 2010, **21**, 328–337.
23. N. J. Treat, D. Smith, C. Teng, J. D. Flores, B. A. Abel, A. W. York, F. Huang and C. L. McCormick, *ACS Macro Lett*, 2011, **1**, 100-104.

24. T. Kanazawa, H. Taki, K. Tanaka, Y. Takashima and H. Okada, *Pharm. Res.*, 2011, **28**, 2130-2139.
25. A. Nori, K. D. Jensen, M. Tijerina, P. Kopečková and J. Kopeček, *J. Controlled Release*, 2003, **91**, 53-59.
26. A. Nori, K. D. Jensen, M. Tijerina, P. Kopečková and J. Kopeček, *Bioconjugate Chem.*, 2002, **14**, 44-50.
27. S. K. Hamilton and E. Harth, *Acs Nano*, 2009, **3**, 402-410.
28. A. Hennig, G. J. Gabriel, G. N. Tew and S. Matile, *J. Am. Chem. Soc.*, 2008, **130**, 10338-10344.
29. Y. Kim, S. Binauld and M. H. Stenzel, *Biomacromolecules*, 2012, **13**, 3418-3426.
30. H. Ringsdorf, *J Polym Sci: Polym Symp*, 1975, **51**, 135-153.
31. N. Larson and H. Ghandehari, *Chem Mater*, 2012, **24**, 840-853.
32. C. E. Hoyle, A. B. Lowe and C. N. Bowman, *Chem Soc Rev*, 2010, **39**, 1355-1387.
33. M. H. Stenzel, *ACS Macro Letters*, 2013, **2**, 14-18.
34. S. H. Thang, Y. K. Chong, R. T. A. Mayadunne, G. Moad and E. Rizzardo, *Tetrahedron Lett*, 1999, **40**, 2435-2438.
35. S. M. Birnbaum, M. Winitz and J. P. Greenstein, *Arch Biochem Biophys*, 1956, **60**, 496-498.
36. J. H. Price, A. N. Williamson, R. F. Schramm and B. B. Wayland, *Inorg. Chem.*, 1972, **11**, 1280-1284.
37. S. A. Kane, H. Sasaki and S. M. Hecht, *J Am Chem Soc*, 1995, **117**, 9107-9118.
38. Y. Chen, G. J. Chen and M. H. Stenzel, *Macromolecules*, 2010, **43**, 8109-8114.
39. C. Boyer, A. Bousquet, J. Rondolo, M. R. Whittaker, M. H. Stenzel and T. P. Davis, *Macromolecules*, 2010, **43**, 3775-3784.
40. S. Perrier, P. Takolpuckdee and C. A. Mars, *Macromolecules*, 2005, **38**, 2033-2036.
41. B. M. Rosen, G. Lligadas, C. Hahn and V. Percec, *Journal of Polymer Science Part A: Polymer Chemistry*, 2009, **47**, 3931-3939.
42. J. Han, B. Zhao, A. Tang, Y. Gao and C. Gao, *Polym Chem*, 2012, **3**, 1918-1925.
43. K. E. Locock, T. D. Michl, J. D. Valentin, K. Vasilev, J. D. Hayball, Y. Qu, A. Traven, H. J. Griesser, L. Meagher and M. Haeussler, *Biomacromolecules*, 2013, **14**, 4021-4031.
44. K. E. S. Locock, T. D. Michl, N. Stevens, J. D. Hayball, K. Vasilev, A. Postma, H. J. Griesser, L. Meagher and M. Haeussler, *ACS Macro Lett*, 2014, **3**, 319-323.
45. Z. Qin, W. Liu, L. Li, L. Guo, C. Yao and X. Li, *Bioconjug Chem*, 2011, **22**, 1503-1512.
46. V. T. Huynh, P. de Souza and M. H. Stenzel, *Macromolecules*, 2011, **44**, 7888-7900.
47. J. ŠebestíK, I. Stibor and J. HlavÁček, *J. Peptide Sci.*, 2006, **12**, 472-480.

